CHINESE OPTICS LETTERS

Vol. 21, No. 6 | June 2023

Environmentally stable, spectral-shape-controllable, GHz femtosecond Yb-doped fiber laser

Kefeng Chen (陈可封)[1], Lina Gan (甘丽娜)[1], Yingge Tao (陶英阁)[1], Weilin Shao (邵炜霖)[1], Wei Yu (余 唯)[1], Haowei Lin (林豪威)[1], Zhiping Cai (蔡志平)[1,2], and Huihui Cheng (程辉辉)[1,2,3*]

[1] Department of Electronic Engineering, Xiamen University, Xiamen 361005, China

[2] Fujian Key Laboratory of Ultrafast Laser Technology and Applications, Xiamen University, Xiamen 361005, China

[3] Shenzhen Research Institute, Xiamen University, Shenzhen 518000, China

*Corresponding author: hhcheng@xmu.edu.cn

Received February 17, 2023 | Accepted March 17, 2023 | Posted Online June 6, 2023

We demonstrate an all-polarization-maintaining (PM) passively mode-locked Yb^{3+}-doped fiber laser (YDFL) with a fundamental repetition rate of 1.3 GHz. The optical spectra of a linearly polarized soliton exhibit different shapes by rotating the fast axis of the fiber optical pigtail of a dispersive dielectric mirror. The oscillator provides a series of laser performance, such as a threshold pump power for continuous wave laser oscillation of 3.1 mW, an optical-to-optical efficiency for mode-locking of 29%, and an integrated relative intensity noise of 0.08%. To the best of our knowledge, this is the first report of >1 GHz ultrafast all-fiber YDFL with PM architecture.

Keywords: highly doped fiber; fiber laser; high repetition rate.
DOI: 10.3788/COL202321.061601

1. Introduction

The development of the femtosecond fiber lasers with pulse repetition rates in the gigahertz regime is of interest and has been driven by the optical frequency combs, nonlinear bioimaging, optical communications, and material processing[1–5]. By employing a high-repetition-rate laser operated at a wavelength of 1035 nm, the ablation-cooled material removal can be implemented, and the technique reduces the needed laser pulse energies for ablation and increases the efficiency of the removal process[6]. Scaling the average power in a high-energy pulse amplifier system, high-repetition-rate ultrashort pulse lasers operated in the 1 μm wavelength range play an essential role in the stacking of a pulse train, where the pulse amplification relies on constructive interference of sequential pulses from a pulse train[7,8]. Harmonic mode-locking[9–11] and self-mode-locking[12], methods based on pulse repetition multiplication external to the cavity[13,14], are capable of achieving up to sub-THz pulse repetition rates. However, fundamental mode-locking is more reliable for some certain applications owing to its high spectral purity and stability. During the last two decades, candidates of active media providing optical gain for gigahertz fundamental repetition rates have been restricted to semiconductors[15–17], rare-earth- (RE) doped ceramic/crystals[18–20], Ti:sapphire crystals[21,22], and glass fibers[23–26]. In contrast, the laser setup constructed with active fibers, i.e., fiber lasers, stands out for its compactness, lack of susceptibility to misalignment, and efficient thermal dissipation. Liu *et al.* reported a femtosecond Yb^{3+}-doped fiber laser (YDFL) with a repetition rate of 750 MHz and a maximum power of 150 mW, which is mode locked by a nonlinear amplifying loop mirror technique[27]. In 2022, Yang *et al.* realized an ultralow timing jitter of 130 as (integrated from 10 kHz–1 MHz) from an 840-MHz nonlinear polarization evolution mode-locked fiber laser[24]. Despite the efforts to enhance the characteristics, repetition rates in these ring-cavity fiber lasers are typically no more than 1 GHz. As for linear resonant-cavity YDFLs, multi-gigahertz repetition rates have been reported both in theories and experiments[27-30].

At higher pulse repetition rates, the tendency for *Q*-switched mode-locking will unavoidably increase[31,32]. The pulse instability, two types of pulsation resulting from gain- and soliton-induced pulse breathing in a GHz-repetition-rate passively mode-locked fiber laser, was numerically investigated[33]. In addition, saturable absorber (SA)-based mode-locked fiber lasers with high repetition rates can easily suffer from temperature-dependent polarization dynamics because the fiber birefringence varies with the ambient temperature[34], and subsequent polarization components interact with each other through nonlinear polarization coupling[35]. In 2021, Lin *et al.* found that by twisting the no-PM gain fiber the soliton dynamics could be induced from linearly polarized solitons (LPSs) to polarization rotation vector solitons in the high-repetition-rate

ultrafast fiber laser [36]. Hitherto, multi-gigahertz fundamentally mode-locked fiber lasers with PM architectures have been rarely reported. In 2022, Ou *et al.* demonstrated a 1.12-GHz repetition-rate YDFL using a PM gain fiber and free-space components in a ring cavity[37]. By employing a piece of Er^{3+}-heavily doped glass fiber, Song *et al.* reported a 1.03-GHz PM fiber laser, which represented an output power of 550 μW with a corresponding optical-to-optical efficiency of 0.3%[38].

Herein, we demonstrated a 1.3 GHz passively mode-locked all-fiber YDFL with an all-PM architecture. To the best of our knowledge, this is the first PM fiber laser with a >1 GHz repetition rate operating in the 1 μm wavelength range. The optical spectral shapes of the LPSs can be controlled by rotating the fast axis of the fiber optical pigtail of the designed dispersive dielectric mirror (DDM). Benefitting from the optimized systemic parameters of the centimeter-scale laser cavity, the optical-to-optical efficiency for the LPSs reached 29%.

2. Experimental Setup

A schematic illustration of an all-PM YDFL with a 1.3 GHz fundamental repetition rate is shown in Fig. 1(a). An 8.8-cm-long PM Yb^{3+}-doped fiber (PM-YDF, Corative YB 401-PM) was used as the gain medium in the Fabry–Pérot-type oscillator. A photograph of the cross section of the PM-YDF is illustrated in Fig. 1(b), showing the fiber core and the stress axis. The PM-YDF has 5/125 μm core/cladding diameters and a numerical aperture of 0.14. The small-signal gain coefficient and the group velocity dispersion (GVD) are 0.76 dB/cm and 238 fs^2/cm at a wavelength of 1040 nm, respectively. Protected by a PM-isolator (PM-ISO) operating at approximately 980 nm, a 976 nm/680 mW laser diode (LD) acts as a pump source through a PM wavelength division multiplexer (PM-WDM) to excite the PM-YDF. In the experiment, all of the fiber optical pigtails of optical devices are panda PM silica fiber (Corning PM980) [the photograph of the cross section is shown in Fig. 1(c)]. The PM-YDF was secured with epoxy in a zirconia ferrule with an inner diameter of 125 μm, and both end facets of the fiber assembly were polished flat. One end of the PM-YDF was butt-coupled to a DDM that was secured by the fiber optical pigtail. The pigtail of the DDM was spliced to the common port of the PM-WDM. The DDM was fabricated by alternately coating SiO_2/Ta_2O_5 dielectric films onto a zirconia ferrule using a plasma sputter deposition system. The DDM exhibits a high transmittance of 98.8% at a pump wavelength of 976 nm, a reflectivity of 89.3%, and a GVD of −761 fs^2 at a wavelength of 1040 nm. As shown in Fig. 1(d), the DDM was deposited on the end facet of the PM-fiber ferrule. The opposite end of the PM-YDF was butted to a semiconductor saturable absorber mirror (SESAM) [Fig. 1(e)], which was sandwiched between the PM-YDF and the zirconia ferrule. The SESAM has a modulation depth of 5%, a non-saturable loss of 3%, a relaxation time of 1 ps, and a saturation fluence of 40 $\mu J/cm^2$ at 1040 nm (Batop GmbH). The reflectivity and the GVD of the SESAM over the 1020–1060 nm wavelength intervals are illustrated in Fig. 1(f). At the laser wavelength of 1040 nm, the reflectivity and the GVD are 91.9% and 72.6 fs^2, respectively. The net GVD of the whole laser cavity is estimated to be 1404 fs^2.

The LPSs with a pulse repetition rate of 1.3 GHz were coupled out via the signal port of the PM-WDM, which was spliced to a

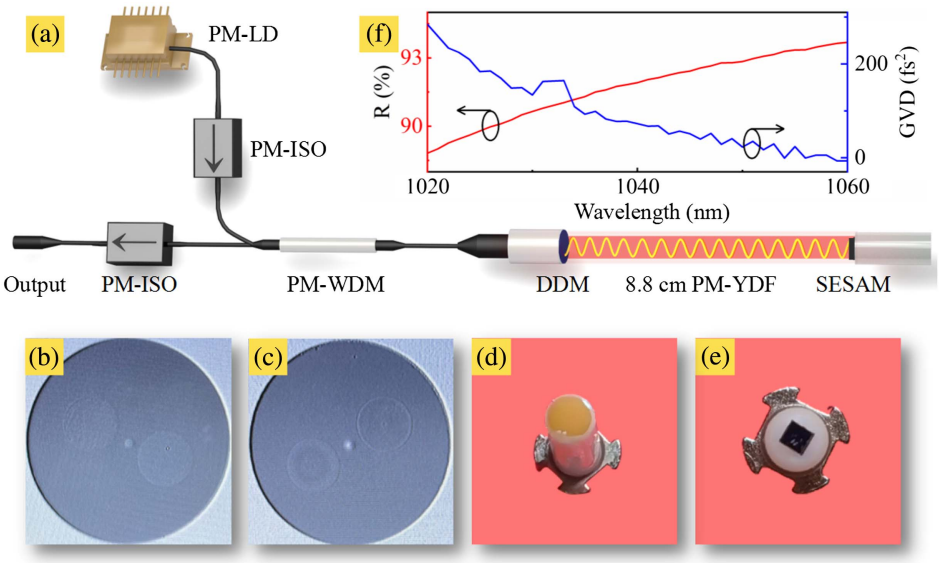

Fig. 1. (a) Schematic illustration of the 1.3-GHz ultrafast YDFL with an all-PM architecture. Polarization-maintaining Yb^{3+}-doped fiber, PM-YDF; laser diode with PM fiber optical pigtail, PM-LD; polarization-maintaining isolator, PM-ISO; polarization-maintaining wavelength division multiplexer, PM-WDM; dispersive dielectric mirror, DDM; semiconductor saturable absorber mirror, SESAM. (b) Photograph of the cross section of the PM-YDF. (c) Photograph of the cross section of the PM passive fiber (Corning PM-980). (d) Photograph of the DDM coated on the end of the PM-fiber ferule. (e) Photograph of the SESAM that was put on the end of the zirconia ferrule. (f) Low intensity spectral reflectance and the GVD of the SESAM between the PM-YDF and the fiber ferrule.

1040 nm PM-ISO. A pair of transmission diffraction gratings was set for de-chirping external to the cavity. The optical spectra were measured by an optical spectrum analyzer (Ando AQ6315B) with a resolution of 0.05 nm. The temporal waveform was detected by using a 25 GHz photodetector (PD) and a 6 GHz bandwidth digital oscilloscope (Tektronix TDS6604). The radio-frequency (RF) spectrum was detected by a signal analyzer (Keysight N9020A), and the noise characteristics of the PM oscillator was recorded by another signal analyzer (Rohde & Schwarz FSWP50). The pulse duration was measured by an autocorrelator (APE pulseCheck USB 50).

3. Results and Discussion

Figure 2 shows the measurements of the average output power of the 1.3 GHz all-PM mode-locked YDF laser as a function of launched pump power. The continuous wave (CW) laser oscillation started at a pump power of $P = 3.1$ mW, which is a considerably low value owing to the high-quality factor Q for the optimized cavity parameters. In the range of $3.1\ \text{mW} \le P \le 30.3\ \text{mW}$, the output power linearly increases. When P is above 30.3 mW, a regime of rectangular-shaped wave packet (RSWP) is attained, and the slope of the output power remains linear[39]. Once P reaches 52.8 mW, self-started LPSs with a fundamental repetition rate of 1.3 GHz can be achieved. Note also that the maximal output power extracted from the miniature all-PM oscillator is 31.4 mW at the launched pump power $P = 109.1$ mW, corresponding to an optical-to-optical efficiency of 29%.

In the regime of the LPS operation, the peak wavelengths of the mode-locked spectra shift toward shorter wavelengths as the launched pump power increases from 64.1 mW to 103.5 mW, as shown in Fig. 3(a). Interestingly, in the process, the peak intensities gradually increase while the "pedestal" component on the edge of the short wavelength of the spectra [indicated by the dashed circle in Fig. 3(a)] obviously weakens and ultimately

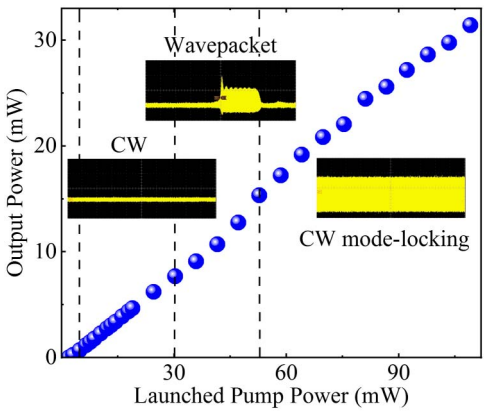

Fig. 2. Measured variation of the average power of the all-PM YDF oscillator with the launched pump power (976 nm). In recording the data, the average power was recorded after the polarization dependent ISO operating at 1040 nm [in Fig. 1(a)].

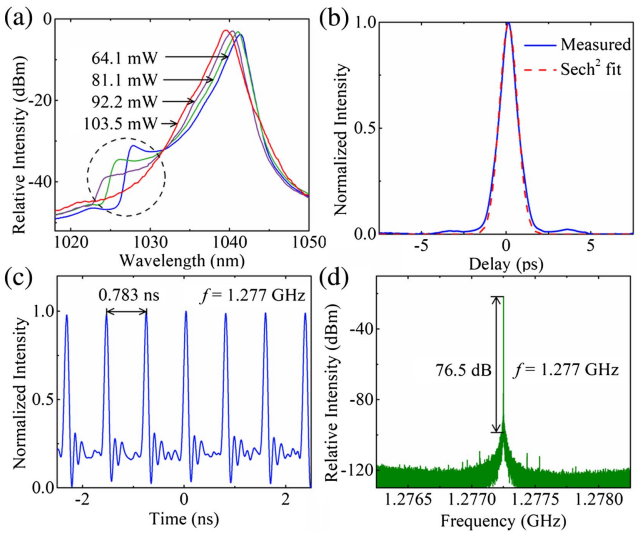

Fig. 3. (a) Spectra of the LPSs observed along the 1040-nm PM-ISO for several values of launched pump power. (b) Autocorrelation trace of the LPSs at a launched pump power of 103.5 mW. (c) Laser waveform measured with an oscilloscope and a photodiode having bandwidths of 6 GHz and 25 GHz, respectively. The interval between the intensity peaks is 783 ps. (d) Spectrum of the photodiode signal in the 1.2762–1.2782 GHz region acquired with an RF spectrum analyzer.

disappears for $P = 103.5$ mW. Moreover, the spectrum displays a peak wavelength of 1040 nm and a spectral width (FWHM) of 1.95 nm. Correspondingly, the measurement of the autocorrelation trace of the de-chirped LPS is shown in Fig. 3(b), indicating a pulse duration of 814 fs and assuming the intensity profile to be hyperbolic secant. Considering a 582-fs transform-limited FWHM pulse duration, the difference can be attributed to a slightly imperfect dispersion compensation. The measurements of the pulse train temporal behavior are shown in Fig. 3(c), illustrating output pulses separated by 783 ps, which corresponds to the fundamental repetition rate of 1.28 GHz. Figure 3(d) shows the radio-frequency spectrum of the all-PM oscillator recorded between 1.2762 GHz and 1.2782 GHz with a 20-Hz resolution bandwidth (RBW). A single peak at 1.28 GHz is observed and the background noise is suppressed by 76.5 dB.

For $P = 103.5$ mW, as shown in Fig. 4(a), the spectral shape of the LPS operation changed [relative to the one in Fig. 3(a)] by rotating the fast axis of the fiber optical pigtail of the DDM, equivalently rotating the angle θ of the fast axis of the DDM to the fast axis of the PM-YDF. The peak wavelength shifts to 1036.6 nm while a "pedestal" component arises on the edge of the long wavelength. In addition, the temporal waveform is shown in the inset of Fig. 4(b), indicating an almost identical intensity of each optical pulse. The RF spectrum measured with a resolution bandwidth (RBW) of 20 Hz in Fig. 4(b) illustrates a signal-to-noise ratio of 77.7 dB and demonstrates that the LPSs with this spectral shape are stable and free of Q-switching instabilities.

The reason for the controllable spectral-shape feature in the LPS laser can be concluded as follows: the radiation of the

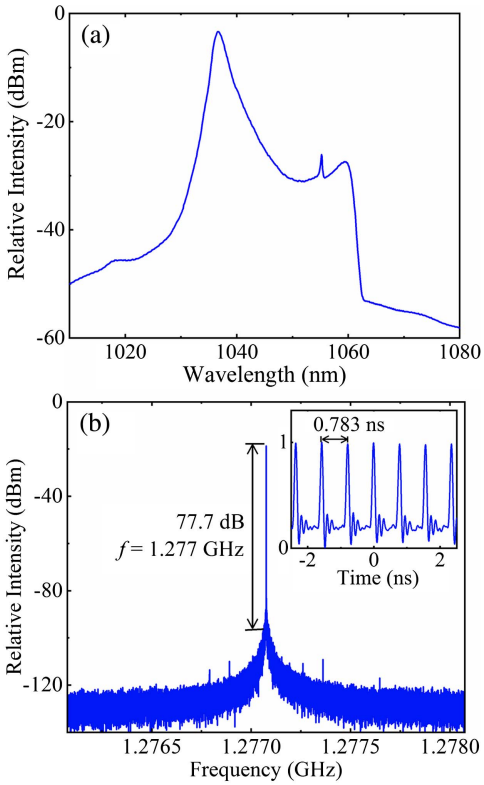

Fig. 4. (a) Mode-locked spectrum of the LPSs by rotating the fast axis of the fiber optical pigtail of the DDM at the launched pump power of 103.5 mW. (b) The corresponding RF spectrum in the 1.2760–1.2780 GHz region. The temporal waveform acquired by an oscilloscope and a photodiode is shown in the inset of (b).

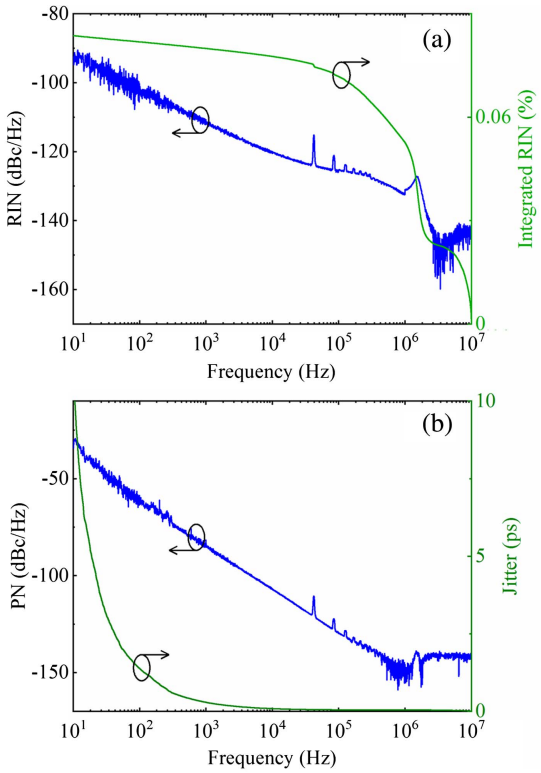

Fig. 5. (a) Relative intensity noise (RIN) (blue curve) of the 1.3 GHz LPS train with the all-PM architecture and integrated RIN (green curve) in the 10 Hz–10 MHz frequency region. (b) The corresponding phase noise (blue curve) and the integrated timing jitter (green).

1.3-GHz pulse train in the resonant cavity is extracted through the fiber–fiber interface from the PM-YDF direction and the PM silica (undoped) fiber direction [Fig. 1(a)]. In the all-PM architecture, each orthogonal component (E_{xo}, E_{yo}) of the LPSs experiences a magnitude change when they pass through the interface and then enter the PM silica fiber because of the existing angle θ of the fast axis of the DDM to the fast axis of the YDF. If we add the emerging E'_{xo} and E'_{yo} with the magnitude change, then the resultant polarization state can be modified by rotating θ. When the light further comes out of the PM-ISO (similar to an analyzer behavior), only the field component parallel to the slow axis will be allowed to pass through. The shape of the optical spectrum therefore relates to the intensity of an LPS passing through a PM-ISO, which can also be modified by the incident polarization state that depended on the angle θ.

We further measured the relative intensity noise (RIN) and the phase noise (PN) of the 1.3 GHz LPSs for $P = 103.5$ mW. While recording the data, the all-PM YDF oscillator did not feature enclosures or any other means to prevent ambient disturbances, such as temperature fluctuation. The RIN (blue curve) and the integrated RIN (green curve) are plotted in the same figure [Fig. 5(a)]. Integration from 10 Hz to 10 MHz results in an integrated RIN of 0.08%. The PN of the all-PM YDFL is shown in Fig. 5(b). The PN gradually decreases from −33 dBc/Hz to −142 dBc/Hz with an increase in an offset frequency from 10 Hz to 10 MHz. The integrated timing jitter is calculated to be 291 fs integrated from 1 kHz to 10 MHz.

4. Conclusion

In summary, a 1.3-GHz YDFL with an all-PM architecture has been demonstrated, and its output spectral shape can be controlled by rotating the angle of the fast axis of the PM-silica fiber of the DDM to the fast axis of the PM-YDF. Owing to optimal systemic parameters, the compact all-fiber PM oscillator exhibits a threshold pump power for a CW laser oscillation of 3.1 mW and an optical-to-optical efficiency for mode locking of 29%. Temperature-dependent polarization dynamics is effectively suppressed in the 8.8-cm all-PM laser cavity, and the relative RIN integrated from 10 Hz to 10 MHz was measured to be 0.08%. The fiber laser emitting high-repetition-rate LPSs described here is readily incorporated into the existing pulse-stacking amplification system as a reliable seed source using coherent addition.

Acknowledgement

This work was supported by the National Natural Science Foundation of China (No. 61905205).

References

1. C.-H. Li, A. J. Benedick, P. Fendel, A. G. Glenday, F. X. Kärtner, D. F. Phillips, D. Sasselov, A. Szentgyorgyi, and R. L. Walsworth, "A laser frequency comb that enables radial velocity measurements with a precision of 1 cm s^{-1}," Nature **452**, 610 (2008).
2. S. Hakobyan, V. J. Wittwer, P. Brochard, K. Gürel, S. Schilt, A. S. Mayer, U. Keller, and T. Südmeyer, "Full stabilization and characterization of an optical frequency comb from a diode-pumped solid-state laser with GHz repetition rate," Opt. Express **25**, 20437 (2017).
3. N. Ji, J. C. Magee, and E. Betzig, "High-speed, low-photodamage nonlinear imaging using passive pulse splitters," Nature **5**, 197 (2008).
4. H. Kalaycıoğlu, P. Elahi, Ö. Akçaalan, and F. Ö. Ilday, "High-repetition-rate ultrafast fiber lasers for material processing," IEEE J. Sel. Top. Quantum Electron. **24**, 8800312 (2018).
5. D. Hillerkuss, R. Schmogrow, T. Schellinger, M. Jordan, M. Winter, G. Huber, T. Vallaitis, R. Bonk, P. Kleinow, F. Frey, M. Roeger, S. Koenig, A. Ludwig, A. Marculescu, J. Li, M. Hoh, M. Dreschmann, J. Meyer, Z. Ben Ezra, N. Narkiss, B. Nebendahl, F. Parmigiani, P. Petropoulos, B. Resan, A. Oehler, K. Weingarten, T. Ellermeyer, J. Lutz, M. Moeller, M. Huebner, J. Becker, C. Koos, W. Freude, and J. Leuthold, "26 Tbit s^{-1} line-rate super-channel transmission utilizing all-optical fast Fourier transform processing," Nat. Photonics **5**, 364 (2011).
6. C. Kerse, H. Kalaycıoğlu, P. Elahi, B. Çetin, D. K. Kesim, Ö. Akçaalan, S. Yavaş, M. D. Aşık, B. Öktem, H. Hoogland, R. Holzwarth, and F. Ö. Ilday, "Ablation-cooled material removal with ultrafast bursts of pulses," Nature **537**, 84 (2016).
7. R. J. Jones and J. Ye, "Femtosecond pulse amplification by coherent addition in a passive optical cavity," Opt. Lett. **27**, 1848 (2002).
8. H. Carstens, N. Lilienfein, S. Holzberger, C. Jocher, T. Eidam, J. Limpert, A. Tünnermann, J. Weitenberg, D. C. Yost, A. Alghamdi, Z. Alahmed, A. Azzeer, A. Apolonski, E. Fill, F. Krausz, and I. Pupeza, "Megewatt-scale average-power ultrashort pulses in an enhancement cavity," Opt. Lett. **39**, 2595 (2014).
9. T. Wang, L. Jin, H. Zhang, W. Pan, H. Zhang, Y. Xu, L. Shi, Y. Li, Y. Zou, and X. Ma, "Gigahertz harmonic mode-locked fiber laser based on tunable SMS ultrafast optical switch," Ann. Phys. **532**, 2000018 (2020).
10. D. Yeh, W. He, M. Pang, X. Jiang, G. Wong, and P. St.J. Russell, "Pulse-repetition-rate tuning of a harmonically mode-locked fiber laser using a tapered photonic crystal fiber," Opt. Lett. **44**, 1580 (2019).
11. Z. Zhao, L. Jin, S. Y. Set, and S. Yamashita, "2.5 GHz harmonic mode locking from a femtosecond Yb-doped fiber laser with high fundamental repetition rate," Opt. Lett. **46**, 3621 (2021).
12. Y.-F. Chen, M.-T. Chang, T.-L. Huang, J.-C. Tung, K. Huang, and H.-C. Liang, "Orthogonally polarized self-mode-locked lasers with repetition rate multiplication up to hundreds of gigahertz: observation of temporal carpets," IEEE J. Sel. Top. Quantum Electron. **24**, 1101806 (2018).
13. X. Li, M. Seghilani, L. R. Cortés, and J. Azaña, "Sub-THz optical frequency comb generation by efficient repetition-rate multiplication of a 250-MHz mode-locked laser," IEEE J. Sel. Top. Quantum Electron. **27**, 7601310 (2021).
14. T. S. Chan and P. Poopalan, "Continuous sub-THz repetition rate CEP-stable ultrashort laser pulses generation via coherent external Fabry–Pérot cavity," IEEE J. Quantum Electron. **57**, 1100307 (2021).
15. N. Jornod, K. Gürel, V. J. Wittwer, P. Brochard, S. Hakobyan, S. Schilt, D. Waldburger, U. Keller, and T. Südmeyer, "Carrier-envelope offset frequency stabilization of a gigahertz semiconductor disk laser," Optica **4**, 1482 (2017).
16. C. G. E. Alfieri, D. Waldburger, J. Nürnberg, M. Golling, and U. Keller, "Sub-150-fs pulses from an optically pumped broadband modelocked integrated external-cavity surface emitting laser," Opt. Lett. **44**, 25 (2019).
17. Y.-W. Song, S. Yamashita, C. S. Goh, and S. Y. Set, "Passively mode-locked lasers with 17.2-GHz fundamental-mode repetition rate pulsed by carbon nanotubes," Opt. Lett. **32**, 430 (2007).
18. A. Barh, B. Ö. Alaydin, J. Heidrich, M. Gaulke, M. Golling, C. R. Phillips, and U. Keller, "High-power low-noise 2-GHz femtosecond laser oscillator at 2.4 μm," Opt. Express **30**, 5019 (2022).
19. S. Kimura, S. Tani, and Y. Kobayashi, "Kerr-lens mode locking above a 20 GHz repetition rate," Optica **6**, 532 (2019).
20. L. M. Krüger, A. S. Mayer, Y. Okawachi, X. Ji, A. Klenner, A. R. Johnson, C. Langrock, M. M. Fejer, M. Lipson, A. L. Gaeta, V. J. Wittwer, T. Südmeyer, C. R. Phillips, and U. Keller, "Performance scaling of a 10-GHz solid-state laser enabling self-referenced CEO frequency detection without amplification," Opt. Express **28**, 12755 (2020).
21. C. Grivas, R. Ismaeel, C. Corbari, C.-C. Huang, D. W. Hewak, P. Lagoudakis, and G. Brambilla, "Generation of multi-gigahertz trains of phase-coherent femtosecond laser pulses in Ti:sapphire waveguides," Laser Photonics Rev. **12**, 1800167 (2018).
22. A. Bartels, D. Heinecke, and S. A. Diddams, "10-GHz self-referenced optical frequency comb," Science **326**, 681 (2009).
23. G. Tang, Z. Liang, W. Huang, D. Yang, W. Lin, L. Tu, D. Chen, Q. Qian, X. Wei, and Z. Yang, "4.3 GHz fundamental repetition rate passively mode-locked fiber laser using a silicate-clad heavily Tm^{3+}-doped germanate core multimaterial fiber," Opt. Lett. **47**, 682 (2022).
24. R. Yang, M. Zhao, X. Jin, Q. Li, Z. Chen, A. Wang, and Z. Zhang, "Attosecond timing jitter from high repetition rate femtosecond "solid-state fiber lasers"," Optica **9**, 874 (2022).
25. J. J. McFerran, L. Nenadović, W. C. Swann, J. B. Schlager, and N. R. Newbury, "A passively mode-locked fiber laser at 1.54 μm with a fundamental repetition frequency reaching 2 GHz," Opt. Express **15**, 13155 (2007).
26. J. Zeng, A. E. Akosman, and M. Y. Sander, "Scaling the repetition rate of thulium-doped ultrafast soliton fiber lasers to the GHz regime," Opt. Express **26**, 24687 (2018).
27. H.-W. Chen, G. Chang, S. Xu, Z. Yang, and F. X. Kärtner, "3 GHz, fundamentally mode-locked, femtosecond Yb-fiber laser," Opt. Lett. **37**, 3522 (2012).
28. I. Hartl, H. A. Mckay, R. Thapa, B. K. Thomas, A. Ruehl, L. Dong, and M. E. Fermann, "Fully stabilized GHz Yb-fiber laser frequency comb," in *Advanced Solid-State Photonics*, OSA Technical Digest Series (Optica, 2009), paper MF9.
29. H. Cheng, W. Wang, Y. Zhou, T. Qiao, W. Lin, Y. Guo, S. Xu, and Z. Yang, "High-repetition-rate ultrafast fiber laser," Opt. Express **26**, 16411 (2018).
30. W. Wang, W. Lin, H. Cheng, Y. Zhou, T. Qian, Y. Liu, P. Ma, S. Zhou, and Z. Yang, "Gain-guided soliton: scaling repetition rate of passively mode-locked Yb-doped fiber lasers to 12.5 GHz," Opt. Express **27**, 10438 (2019).
31. H. Haus, "Parameter ranges for CW passive mode locking," IEEE J. Quantum Electron. **12**, 169 (1976).
32. C. Hönninger, R. Paschotta, F. Morier-Genoud, M. Moser, and U. Keller, "Q-switching stability limits of continuous-wave passive mode locking," J. Opt. Soc. Am. B **16**, 46 (1999).
33. H. Cheng, W. Lin, Y. Zhang, M. Jiang, and W. Luo, "Numerical insights into the pulse instability in a GHz repetition-rate thulium-doped fiber laser," J. Light. Technol. **39**, 1464 (2021).
34. H. Byun, M. Y. Sander, A. Motamedi, H. Shen, G. S. Petrich, L. A. Kolodziejski, E. P. Ippen, and F. X. Kärtner, "Compact, stable 1 GHz femtosecond Er-doped fiber laser," Appl. Opt. **49**, 5577 (2010).
35. D. N. Christodoulides and R. I. Joseph, "Vector solitons in birefringent nonlinear dispersive media," Opt. Lett. **13**, 53 (1988).
36. W. Lin, W. Wang, B. He, X. Chen, X. Hu, Y. Guo, Y. Xu, X. Wei, and Z. Yang, "Vector soliton dynamics in a high-repetition-rate fiber laser," Opt. Express **29**, 12049 (2021).
37. S. Ou, Z. Yu, L. Guo, Q. Zhang, N. Zhang, H. Liu, and P. P. Shun, "GHz-repetition-rate fundamentally mode-locked, isolator-free ring cavity Yb-doped fiber lasers with SESAM mode- locking," Opt. Express **30**, 43543 (2022).
38. J. Song, X. Hu, H. Wang, T. Zhang, Y. Wang, Y. Liu, and J. Zhang, "All-polarization-maintaining, semiconductor saturable absorbing mirror mode-locked femtosecond Er-doped fiber laser with a gigahertz fundamental repetition rate," Laser Phys. Lett. **16**, 095102 (2019).
39. H. Cheng, W. Wang, Y. Zhou, T. Qiao, W. Lin, S. Xu, and Z. Yang, "Investigation of rectangular shaped wave packet dynamics in a high-repetition-rate ultrafast fiber laser," Opt. Express **25**, 20125 (2017).